Supercond. Sci. Technol. **20** (2007) S467–S471 doi:10.1088/0953-2048/20/11/S32

# Phase evolution in PLD $MgB_2$ films during the *in situ* annealing process

**Y Zhao[1], Y S Wu[1], C Kong[2], D Wexler[1], M Vos[3], M R Went[3] and S X Dou[1]**

[1] Institute for Superconducting and Electronic Materials, University of Wollongong, Wollongong, NSW 2522, Australia
[2] Electron Microscopy Unit, University of New South Wales, Sydney, NSW 2000, Australia
[3] Research School of Physical Sciences and Engineering, Australian National University, Canberra, ACT 0200, Australia

Received 15 June 2007, in final form 7 August 2007
Published 18 October 2007
Online at stacks.iop.org/SUST/20/S467

**Abstract**
The transformation of zero-field-cooled (ZFC) magnetization curves of PLD $MgB_2$ films annealed *in situ* for different dwell times and at different temperatures is studied within the context of structural analysis. The PLD films were deposited using an off-axis geometry followed by two series of annealing conditions: the dwell time series and the annealing temperature series. ZFC magnetization curves were obtained in an MPMS magnetometer from samples that had been cut into similar shapes. XRD scans on the two series of film samples show enhanced (001) and (002) $MgB_2$ peaks till a dwell time of 9 min at a 650 °C and a 800 °C annealing temperature. TEM results show a granular transformation from an un-annealed film to a 700 °C 9 min *in situ* annealed film. The possible structural development with annealing time and annealing temperature is then discussed.

(Some figures in this article are in colour only in the electronic version)

## 1. Introduction

The discovery of superconductivity in $MgB_2$ has attracted a great deal of interest in exploring its adaptability to superconducting electronics applications, due to its relatively high transition temperature, long coherence length and simple chemical structure [1–7]. The two-gap feature of $MgB_2$ also enables it to have a great variability in the performance of $MgB_2$ electronics with different microstructures and doping levels [6]. The platform for $MgB_2$ electronics—thin films of $MgB_2$—is of crucial importance to the device performance. Due to Mg's extraordinary reactivity with oxygen, the $MgB_2$ thin film preparation technology has been mainly based on physical vapor deposition methods, such as pulsed laser deposition with *ex situ* annealing [8, 9] and *in situ* annealing [10], molecular beam epitaxy MBE [11], sputtering [12, 13], hybrid physical–chemical vapor deposition (HPCVD) [14] and reactive evaporation [15]. Among them, HPCVD and reactive evaporation methods generate perhaps the best combination of $T_c$ (about 40 K), epitaxy (in-plane aligned), surface smoothness ($R_{ms} \sim 3$ nm) and reproducibility.

The difficulty of $MgB_2$ film preparation comes from the highly divergent vapor pressures of the Mg and B, and the oxidization of Mg. However, this problem seems well solved by a carefully sealed deposition chamber and a continuous Mg vapor supply to the film surface at elevated temperatures of about 700 °C in both HPCVD and reactive evaporation methods. For electronics applications, such as Josephson junctions (JJ), the surface/interface quality of each layer is another influential factor for reliable performance. With a high temperature as-grown routine in both the above-mentioned methods, the film surfaces were characterized with a planar growth feature and are qualified for electronic applications.

The $MgB_2$ film study in our group has been focused on the *in situ* annealing of $MgB_2$ films with an off-axis geometry of the PLD deposition. The PLD method is readily available among the superconducting laboratories and industry around the world, and is closely linked with electronics fabrication procedures. The off-axis deposition geometry solves the commonly existing problem of surface particulates in on-axis $MgB_2$ films [16]. Although the $T_c$ of *in situ* annealed films is substantially suppressed, the pinning in the *in situ* films is very strong and shows a nanosized granular microstructure. These

  

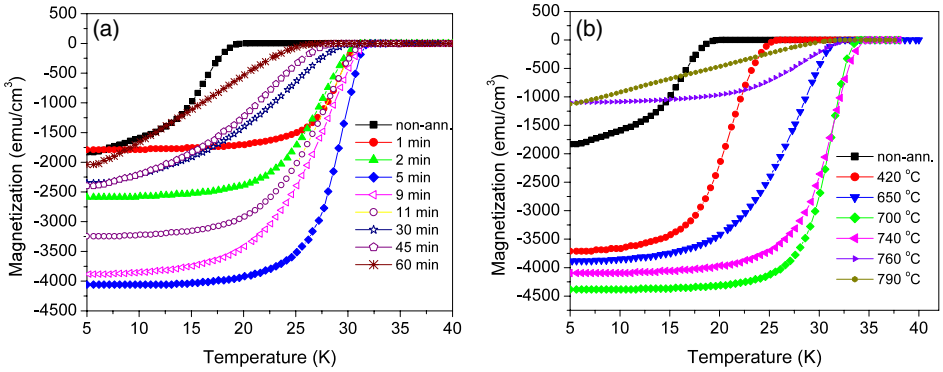


**Figure 1.** Magnetization curves of two series of films: (a) the annealing temperature fixed at 650 °C and (b) the annealing time fixed at 9 min.

features may have some potential usage in those electronics systems where pinning is required. In this paper we further develop our research on the *in situ* annealed off-axis $MgB_2$ films by studying the phase evolution with annealing times and with increasing annealing temperature. The $T_c$ has been significantly improved to 34 K in this study and we are looking forward to a bulk-like $T_c$ in this kind of off-axis PLD film in the future.

## 2. Experimental details

The off-axis films were deposited at 250 °C in 120 mTorr Ar from a stoichiometric $MgB_2$ target. The target was hot-press prepared with 84% density and 99% purity. The 250 mJ/pulse KrF laser beam ($\lambda = 248$ nm) trimmed from the 500 mJ/pulse original beam was focused to a 7 mm$^2$ spot on the target. The substrate surface was aligned parallel to the axis of the plume during the deposition. The average distance between the target and the substrate is about 25 mm. The $MgB_2$ deposition lasted for 15 min at 10 Hz pulse frequency and then the target was switched to the pure Mg target and an Mg cap layer was deposited for 6 min to compensate for the Mg loss during the following annealing. For details of the off-axis preparation of superconducting $MgB_2$ films, also see [16].

We chose different dwell times and annealing temperatures in two series of film annealing experiments. In the first series, the annealing temperature was fixed at 650 °C and the dwell time of the annealing varied from 1 to 60 min. In the second series, the dwell time was fixed at 9 min, and the annealing temperatures were set between 420 and 790 °C. During the annealing, the vacuum chamber was filled with 1 atm high purity Ar.

The magnetic transition curves were measured in a Quantum Design MPMS magnetometer in a ZFC state under a perpendicularly applied field $B_a$ of 25 Oe. The thickness of the films was carefully measured using a scanning electron microscope to calculate the magnetization values. Since the film specimens for the magnetization measurement have similar dimensions (about 5 mm × 2 mm × 500 nm), we believe that the intensity of magnetization reveals the proportion of the superconducting phase in the films.

The transmission electron microscope (TEM) specimen of the selected films was prepared by a focused ion beam with a thickness of 80–100 nm. The TEM observation was carried out in a JEOL JEM200 TEM machine. The selected-area electron diffraction (SAED) images were obtained using a 200 nm area selecting aperture. The XRD $2\theta$ scan was done in a MAC Scientific goniometer operating with Cu K$\alpha$ x-rays. The scanning rate was kept at a very low value of 0.2° min$^{-1}$ for all the samples. We used a novel nondestructive surface content-detecting method, electron Rutherford backscattering spectroscopy (ERBS), to reveal the magnesium oxide surface layer in a typical film. For a detailed description of ERBS, see [17, 18].

## 3. Results and discussions

Shown in figure 1 are the magnetization curves of the films prepared by the two series of annealing conditions. In the time series (figure 1(a)) there is a quite clear trend that the magnetization value at 5 K increases with the dwell time at 650 °C till 5 min. Further prolongation of the dwell time leads to a decrease of the magnetization value and a broadened transition width. It is worth noting that the samples annealed between 1 and 11 min show a quite consistent $T_{c\ onset}$s of 31–32 K, and the decease of $T_{c\ onset}$ for samples annealed for longer times is not dramatic. The slow drop of $T_c$ indicates that there is not a crucial decomposition reaction at that temperature: rather, it may be due to the gradual, diffusive reaction between the $MgB_2$ film and the residual oxygen in the atmosphere or the sapphire substrate. The vacuum chamber used in this study is not of ultra-high vacuum (UHV) standard and we expect better crystallization and $T_c$ in our new UHV PLD system under construction with very low oxygen contamination and thus prolonged dwell time.

When we fix the annealing time at 9 min and gradually increase the annealing temperature, the $T_{c\ onset}$ also increases gradually for the films annealed at temperatures up to 700 °C, as shown in figure 1(b). The film annealed at 740 °C has a similar transition curve with the 700 °C film, the $T_{c\ onset}$s of both films are over 34 K with a narrow transition width of about 6 K. Slightly higher annealing temperatures of 760 and 790 °C result in dramatically decreased magnetization values at 5 K, as well as too wide transition widths, which makes us believe that the decomposition temperature of $MgB_2$ phase falls in between 740 and 760 °C, under our annealing conditions.

Compared with the previous study on the *in situ* annealing conditions for on-axis PLD $MgB_2$ films [19], the optimal

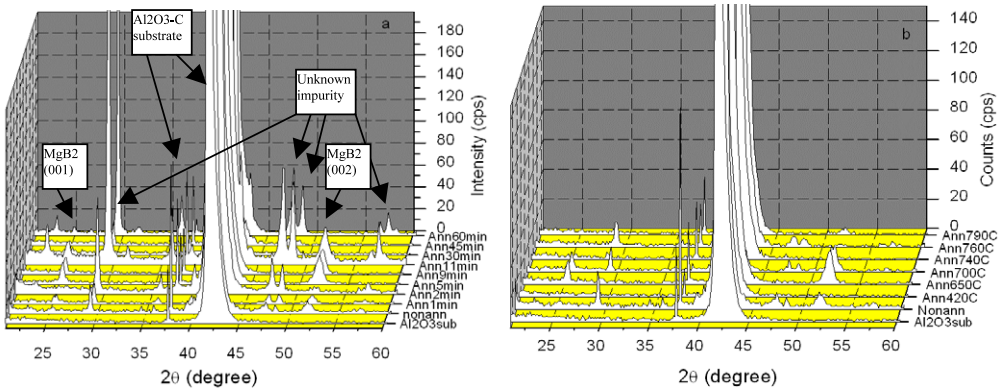


**Figure 2.** X-ray diffraction spectra of the samples prepared at different conditions: (a) annealed at 650 °C with different annealing times. (b) Annealed at different temperatures for 9 min. The XRD scan employed a very low scan rate, 0.2° $min^{-1}$, to reveal the weak x-ray signals from the thin film. The peaks of (001) and (002) reveal *c*-orientation in the series off-axis films.

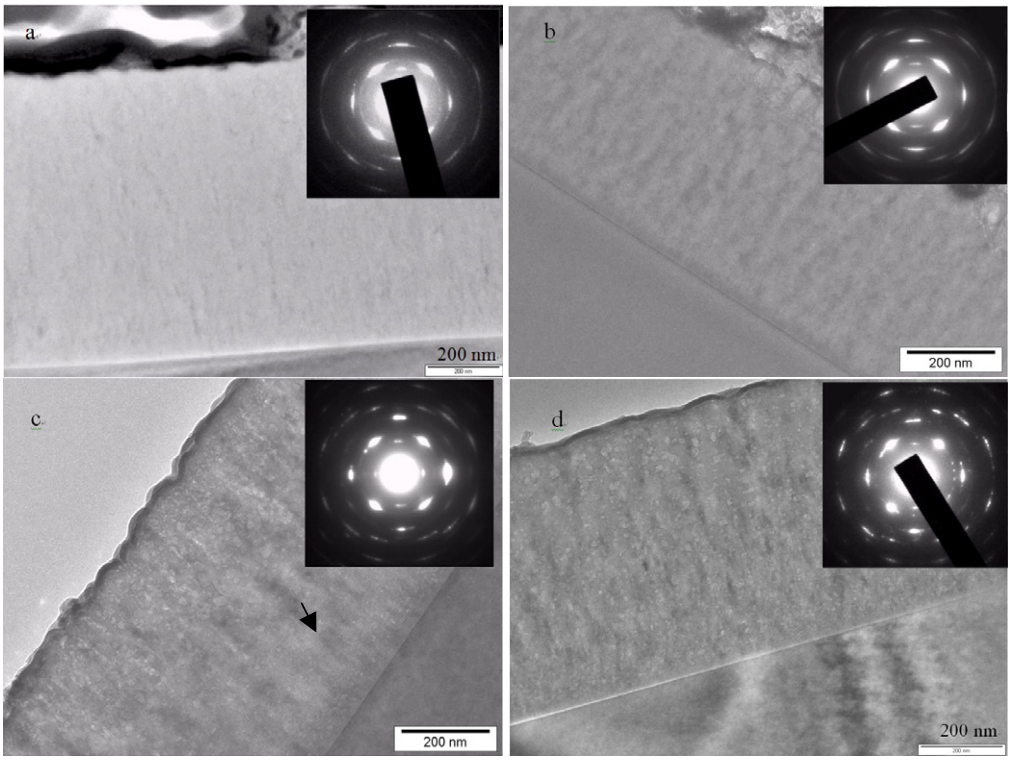


**Figure 3.** TEM cross-sectional bright field images of (a) the un-annealed precursor, (b) 450 °C annealed for 9 min, (c) 650 °C annealed for 1 min and (d) 700 °C annealed for 9 min films. The inset figures are SAED patterns of the films generated from an Φ 200 nm area in the middle of the cross section of each film.

dwell time is longer for the off-axis deposited films (5–9 min for the off-axis film and only 1 min for the on-axis film), while the optimal annealing temperature is similar in the two circumstances. The similar optimal annealing temperatures represent the best crystallization condition while maintaining the $MgB_2$ film safe from decomposition. The reason that the off-axis deposited film achieves the maximum $T_c$ with a longer annealing time may lie in the fact that the off-axis precursor film is of lower defect level than the on-axis film due to the slow growth rate and the absence of droplets in the film. It was also noted that the $MgB_2$ phase formation in the as-deposited off-axis film is better than the on-axis film, which is not superconducting. This makes for a better crystallization during the annealing with a long dwell time possible in the off-axis precursor films, due to the low level of microscopic defects. As a result, the best annealed off-axis film possesses a significantly improved $T_c$, which is 5 K higher than that for the best on-axis film.

XRD $\theta$–$2\theta$ scans on the two series films show the strongest $MgB_2$ (001) and (002) peaks in the films annealed for 5 to 11 min in the time series (figure 2(a)), and in those annealed at 650 and 700 °C in the temperature series (figure 2(b)). This trend is in accordance with the strongest magnetization signals found in these films at 5 K. Significant

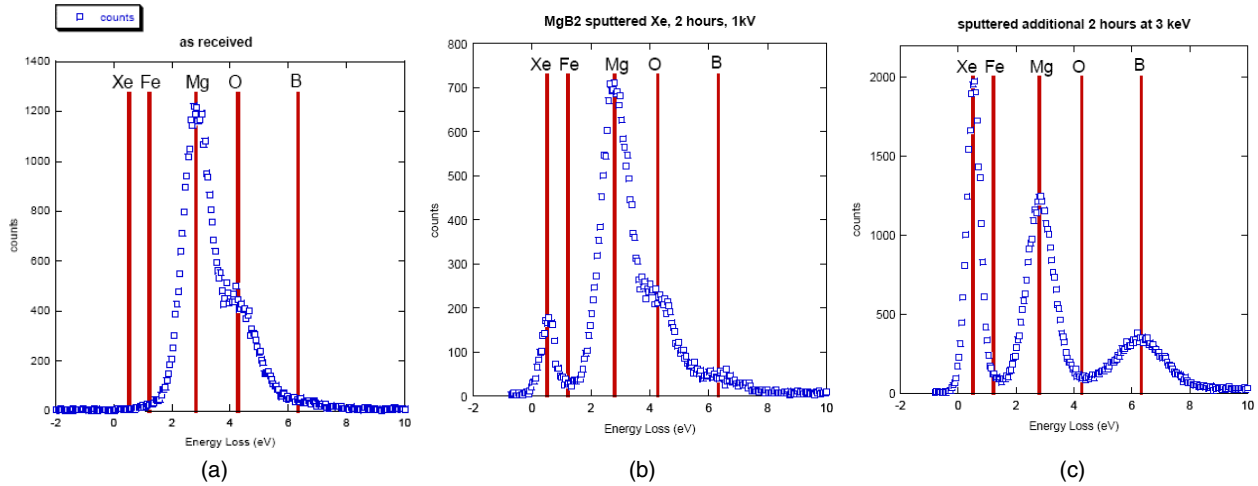


**Figure 4.** Electron Rutherford backscattering spectrum of a 650 °C 1 min annealed film. (a) Original sample, (b) with 2 h low-energy 1 keV Xe ion sputtering and (c) with further 2 h higher-energy 3 keV Xe ion sputtering.

impurity peaks from unknown phase(s) are also seen in most of the XRD scans. Our fitting shows these peaks could all come from a calcite-structured phase (like $CaCO_3$). As will be discussed later in this paper, we assume these peaks reveal an oxygen-rich phase with the calcite structure on top of most of our films.

Figure 3 shows the TEM cross section of four typical $MgB_2$ films studied previously: (a) the un-annealed precursor, (b) 450 °C annealed for 9 min, (c) 650 °C annealed for 1 min and (d) 700 °C annealed for 9 min. With the increase of annealing time and temperature the films show more granular features. It appears that the increase of temperature is more effective than the extension of annealing time in boosting the crystallization. That explains why, after annealing at 420 °C for 9 min, the $T_c$ of the film was only slightly increased, while at 650 °C annealing for as little as 1 min provides similar $T_c$ as those longer-time annealed ones. On the other hand, the similarly high magnetization values of the films annealed at 420–740 °C for a relatively long annealing time of 9 min (figure 1(b)) might indicate that a homogeneous phase formation and crystallization throughout the films was achieved by a suitably prolonged dwell time. In turn, the low 5 K magnetization values of briefly annealed films are evident for an incomplete/localized phase formation and crystallization due to the lack of time. This localized crystallization is clearly seen in the TEM bright field image of the 1 min annealed film shown in figure 3(c)—compared with the 9 min annealed film shown in figure 3(d), the grains appear of various sizes and the arrowed part does not show granular features at all. The SAED patterns shown in figure 3 insets coincide with our above-mentioned arguments. That is, the diffraction signals from $MgB_2$ in the low-temperature/long-time annealed film (figure 3(b)) is even and continuous while the high-temperature/short-time annealed film (figure 3(c)) shows a combination of scattered and continuous signals in the pattern. Only the high-temperature/long-time annealed film (figure 3(d)) illustrates a predominantly scattered SAED pattern. The symmetric distribution of the SAED patterns instead of a ring shape indicates a *c*-axis orientation of the films, which is in accordance with the XRD results.

The last issue we are going to discuss in this paper is the origin of the impurity peaks picked up by the XRD $\theta$–$2\theta$ scans. Figure 4 shows ERBS analysis on the surface of a 650 °C 1 min annealed film. The spectrum for the original film surface shows a significant amount of oxygen in the original film in (a). With 2 h low-energy 1 keV Xe ion sputtering of the original film surface, the oxygen step still remains, and a slight boron peak starts to present in (b). With further 2 h higher-energy 3 keV Xe ion sputtering, the oxygen step becomes unnoticeable, only Mg, B and the residual Xe were detected in (c). The ERBS result clearly shows that a surface oxidized layer is on top of the fairly pure $MgB_2$ film matrix. Judging from the persistence of the oxygen under Xe ion sputtering, the surface oxide layer could be as thick as 100 nm. The oxide layer at the film surface, which may come from the reaction with the residual oxygen in the annealing atmosphere, can present problems for electronics applications and should be eliminated. However, if the thickness and homogeneity of this oxide layer could be controlled, it may also be utilized as a barrier layer for JJ. Further investigations on the $MgB_2$ film surface oxidization using ERBS method will be published elsewhere.

## 4. Conclusions

The phase formation of the off-axis PLD $MgB_2$ films depends crucially on the *in situ* annealing temperature and the annealing time. The optimal annealing temperature appears to be 700–740 °C and the annealing time about 5–9 min in 1 atm Ar atmosphere. XRD shows the strongest $MgB_2$ (001) and (002) peaks under those optimal conditions. Peaks from impurity phases are shown in different films. ERBS results confirm that the impurity detected by XRD only exists along the film surface and contains large amount of oxygen. TEM showed a granular transformation in the *in situ* films with the increase of the annealing temperature and dwell time.

## Acknowledgments

This work was supported in part by the Australian Research Council under Discovery Project DP0666853. YZ thanks Dr Z X Chen and Professor P Munroe for their support of

the TEM work in this paper and Dr Jia Du and Professor E W Collings for their useful discussions.

## References


[1] Nisenoff M 2001 An assessment of superconducting digital technology: the possible impact of the discovery of magnesium diboride *High Tc Update* http://www.iitap.iastate.edu/htcu/nisenoffcomment.html

[2] Ueda K and Naito M 2002 Tunnel junctions on as-grown superconducting $MgB_2$ thin films *Preprint* cond-mat/0208571

[3] Saito A, Kawakami A, Shimakage H and Wang Z 2002 Fabrication of Josephson junctions with as-grown $MgB_2$ thin films *ASC 2002: Superconductors in the Marketplace*

[4] Plecenik A, Kus P, Satrapinsky L, Xu Y and Sobolewski R 2002 Fabrication and transport properties of $MgB_2$ thin films and tunnel junctions *J. Supercond. Incorporating Novel Magn.* **15** 621

[5] Mijatovic D 2004 $MgB_2$ thin films and Josephson devices *PhD Thesis* University of Twente

[6] Dahm T and Scalapino D J 2004 Nonlinear microwave response of $MgB_2$ *Appl. Phys. Lett.* **85** 4436

[7] Booth J *et al* 2003 Nonlinear microwave response of $MgB_2$ thin films *Supercond. Sci. Technol.* **16** 1518–22

[8] Kang W N *et al* 2001 $MgB_2$ superconducting thin films with a transition temperature of 39 K *Science* **292** 1521

[9] Eom C B *et al* 2001 High critical current density and enhanced irreversibility field in superconducting $MgB_2$ thin films *Nature* **411** 558–60

[10] Zeng X H *et al* 2001 Superconducting properties of nanocrystalline $MgB_2$ thin films made by an *in situ* annealing process *Appl. Phys. Lett.* **79** 1840–2

[11] Ueda K and Naito M 2001 As-grown superconducting $MgB_2$ thin films prepared by molecular beam epitaxy *Appl. Phys. Lett.* **79** 2046

[12] Vaglio R, Maglione M G and Capua R D 2002 High-quality $MgB_2$ thin films *in situ* grown by dc magnetron sputtering *Supercond. Sci. Technol.* **15** 1236

[13] Saito A, Kawakami A, Shimakage H and Wang Z 2002 As-grown deposition of superconducting $MgB_2$ thin films by multiple-target sputtering system *Japan. J. Appl. Phys.* **41** L127–9

[14] Zeng X H *et al* 2003 Superconducting $MgB_2$ thin films on silicon carbide substrates by hybrid physical–chemical vapor deposition *Appl. Phys. Lett.* **82** 2097–9

[15] Moeckly B H 2005 *IEEE Trans. Appl. Supercond.* **15** 3308

[16] Zhao Y, Ionescu M, Horvat J and Dou S X 2005 Off-axis $MgB_2$ films using an *in situ* annealing pulsed laser deposition method *Supercond. Sci. Technol.* **18** 395–9

[17] Went M R and Vos M 2007 Investigation of binary compounds using electron Rutherford backscattering *Appl. Phys. Lett.* **90** 072104

[18] Went M R and Vos M 2006 Effects of bonding on the energy distribution of electrons scattered elastically at high momentum transfer *Phys. Rev.* B **74** 205407

[19] Zhao Y, Ionescu M, Pan A V and Dou S X 2003 *In situ* annealing of superconducting $MgB_2$ films prepared by pulsed laser deposition *Supercond. Sci. Technol.* **16** 1487